



# **Engineered Emissivity of Textile Fabrics by the Inclusion of Ceramic Particles**

**Dr. David Anderson, Matthew Pooley, Haskell Beckham and Dr. James F Brennan**

# Engineered emissivity of textile fabrics by the inclusion of ceramic particles

Matthew A. Pooley,<sup>1,\*</sup> David M. Anderson,<sup>2</sup> Haskell W. Beckham,<sup>3</sup>  
and James F. Brennan III<sup>4</sup>

<sup>1</sup>Electrical Engineering and Computer Science, Exponent, Inc., 420 Lexington Avenue, Suite 1740, New York, New York 10170, USA

<sup>2</sup>Thermal Sciences, Exponent, Inc., 3350 Peachtree Road NE, Suite 1125, Atlanta, Georgia 30326, USA

<sup>3</sup>Polymer Science and Materials Chemistry, Exponent, Inc., 3350 Peachtree Road NE, Suite 1125, Atlanta, Georgia 30326, USA

<sup>4</sup>Electrical Engineering and Computer Science, Exponent, Inc., 3350 Peachtree Road NE, Suite 1125, Atlanta, Georgia 30326, USA

\*mpooley@exponent.com

**Abstract:** Composite textile materials, created from a blend of different fibers, have long been used to engineer the properties and performance of fabrics to combine comfort with functionality, such as to create materials with differing optical properties. Some changes to the optical properties of materials in the infrared are subtle and difficult to measure. We present a measurement technique, experimental apparatus, and associated data analysis procedure for detecting small changes in the emissivity of fabrics in the mid-infrared wavelength range (7.5–14  $\mu\text{m}$ ). Using this technique, we demonstrate that the emissivity of polyester fabric can be engineered controllably via the inclusion of ceramic microparticles within the fabric fibers.

©2016 Optical Society of America

**OCIS codes:** (110.3175) Infrared imaging; (110.6820) Thermal imaging; (120.6810) Thermal effects.

---

## References and links

1. S. B. Warner, *Fiber Science* (Prentice Hall, 1995), pp. 213–229.
2. W. H. Hills, “Apparatus for making profiled multi-component yarns,” US Patent, No: 5344297 (1994).
3. X. Hu, M. Tian, L. Qu, S. Zhu, and G. Han, “Multifunctional cotton fabrics with graphene/polyurethane coatings with far-infrared emission, electrical conductivity, and ultraviolet-blocking properties,” *Carbon* **95**, 625–633 (2015).
4. ISO 20473:2007(E), *Optics and Photonics – Spectral Bands*, (International Organization for Standardization, 2007).
5. F. P. Incropera and D. P. Dewitt, *Fundamentals of Heat and Mass Transfer*, 5th ed (John Wiley & Sons, 2002), pp. 713–717.
6. D. D. Horinek and M. E. Foumberg, “Lightweight x-ray and gamma radiation shielding fibers and compositions,” US Patent Application Publication, No: 2013/0045382 A1 (2013).
7. ASTM D1777–96 (2015), *Standard Test Method for Thickness of Textile Materials*, (ASTM International, 2015).
8. ASTM D3776 / D3776M–09 (2013), *Standard Test Methods for Mass Per Unit Area (Weight) of Fabric*, (ASTM International, 2013).
9. S. Schleimann-Jensen and K. Forsberg, *New Test Method for Determination of Emissivity and Reflection Properties of Protective Materials Exposed to Radiant Heat* (ASTM International, 1986).

---

## 1. Introduction

Optical properties of textile fibers can be modified by incorporating a large variety of dyes and other additives, varying the fiber cross-sectional shape, or co-spinning of multi-materials [1,2]. The optical properties of the fabrics constructed from fibers are related to the fiber optical properties. While this has been extensively studied for optical properties in the visible region, less has been published on the optical properties of fabrics and other engineered fibrous structures in the infrared regime. Optical properties of fabrics in the infrared regime

are of current commercial interest. Manipulation of the infrared absorption and emission characteristics of fabrics may find applications across a range of different fields, for example in radiative heat management systems that require flexible surfaces or in thermal camouflage coverings.

In the work presented in this article, the infrared optical effects resulting from incorporation of ceramic particles within polyester fibers utilized in textile fabrics were studied. In particular, changes in the mid-infrared (MIR) emissivity of fabrics that are knitted with differing amounts of ceramic-bearing fibers were investigated. Specifically, we developed a method to measure the emission of textile fabrics between 7.5 and 14  $\mu\text{m}$ . While this region is sometimes referred to as the far-infrared (FIR), especially in the textile field [3], we are using the ISO definition of the divisions of the infrared spectrum [4], and therefore will refer to this region as the MIR in this report. The method we present incorporates spatially resolved radiance imaging and data analysis techniques to enable increased sensitivity when measuring small differences in emissivity between samples.

The amount of radiation emitted from an object at a given temperature,  $T$ , is proportional to the emissivity,  $\epsilon$ , of the surface. Ideal emitters, known as black bodies, have an emissivity of 1 and emit a power spectrum as a function of wavelength,  $\lambda$ , described by Planck's law [5]

$$P(\lambda, T) = \frac{2hc^2}{\lambda^2 \left( \exp\left(\frac{hc}{k_B T}\right) - 1 \right)}, \quad (1)$$

where  $h$ ,  $c$ , and  $k_B$  are the Planck constant, the speed of light in a vacuum, and Boltzmann's constant, respectively. The radiance of a black body,  $W_b$ , is given by the integral of the power spectrum,  $W_b = \int P(\lambda, T) d\lambda$ .

Non-ideal emitters, such as the fabric samples in this study, have an emissivity of  $0 < \epsilon < 1$ , which may vary with temperature and wavelength. If the ranges of wavelengths and temperatures under investigation are narrow compared to the spectral variability of the object, a useful approximation is to assume that the object is a grey body and exhibits a temperature-dependent radiance given by

$$W_g(T) = \epsilon W_b(T). \quad (2)$$

The radiance of an object is thus determined by both the object temperature and its emissivity. Consequently, manipulation of an object's emissivity enables the total radiated power of an object at a given temperature to be varied.

In the present study, we approximate textile fabrics as grey body emitters and test this assumption over temperature ranges of interest. We measure fabrics that were engineered to have varying degrees of emissivity in the MIR and show that, by including ceramic particles in the core of the fibers used in the fabric, the MIR emissivity can increase over 2%. We observed a statistically significant positive correlation between the amount of ceramic-bearing fibers added to the fabric and the increase in emissivity.

## 2. Sample information

Fabric samples, made from fibers produced by Hologenix, LLC (Santa Monica, CA), contained varying amounts of ceramic-bearing polymeric fibers. These specialty fibers are similar in construction to multimode optical fibers, except the core of the fiber is a blend of polyethylene terephthalate (PET, i.e., polyester) and ceramic particles (e.g., titanium dioxide), and the cladding of the fiber, which dictates visual appearance and shields the fiber core [6], is PET. Fabrics were knitted using differing amounts of the ceramic-containing fibers to produce fabrics with three different compositions, along with a control fabric that contained no added specialty fibers. All the fabrics were reported to contain 8% elastane fibers, with the

remaining 92% made from polyester or a blend of polyester and ceramic-containing polyester fibers. The fabrics were nominally identical except for the percentage of ceramic-containing polyester fibers.

The ceramic content of the fabrics was measured using an ash analysis technique. Approximately 2 g of each fabric was heated in air at 850°C for 2.5 hours to burn off the polyester and elastane fibers. The mass remaining was composed of the inorganic material contained by the samples. The increased percentage mass remaining of the three ceramic-bearing samples, compared with that of the control sample, gives the percentage mass of these fabrics due to the additional ceramic particles. Table 1 shows the ceramic content, along with the thickness, measured in general accordance with the American Society for Testing and Materials (ASTM) standard ASTM D 1777 [7] under a mass delivering 0.045 g/mm<sup>2</sup> of pressure, and the basis weight, measured in general accordance with ASTM D 3776 [8] for each of the four sample fabrics.

**Table 1. Physical Properties of Sample Fabrics <sup>a</sup>**

| Sample No. | Thickness (mm) <sup>b</sup> | Basis weight (g/m <sup>2</sup> ) <sup>c</sup> | Ceramic content (% mass) |
|------------|-----------------------------|---|--------------------------|
| 1          | 0.58                        | 152   | 1.22 ± 0.04              |
| 2          | 0.58                        | 152   | 1.03 ± 0.06              |
| 3          | 0.59                        | 156   | 0.53 ± 0.03              |
| 4          | 0.58                        | 150   | 0                        |

<sup>a</sup>Sample 4 is the control and contains no ceramic material; samples 3 to 1 contain increasing amounts of ceramic material as indicated. Errors bars are derived from the standard deviation of multiple measurements.

<sup>b</sup>Thickness was measured under a compression of 0.045 g/mm<sup>2</sup>; standard deviations are ≤ 0.01 mm.

<sup>c</sup>Standard deviations are ≤ 3 g/m<sup>2</sup>.

Optical microscopy was used to confirm that all the fabric samples exhibited the same color, knit structure, and texture, as shown in Fig. 1.

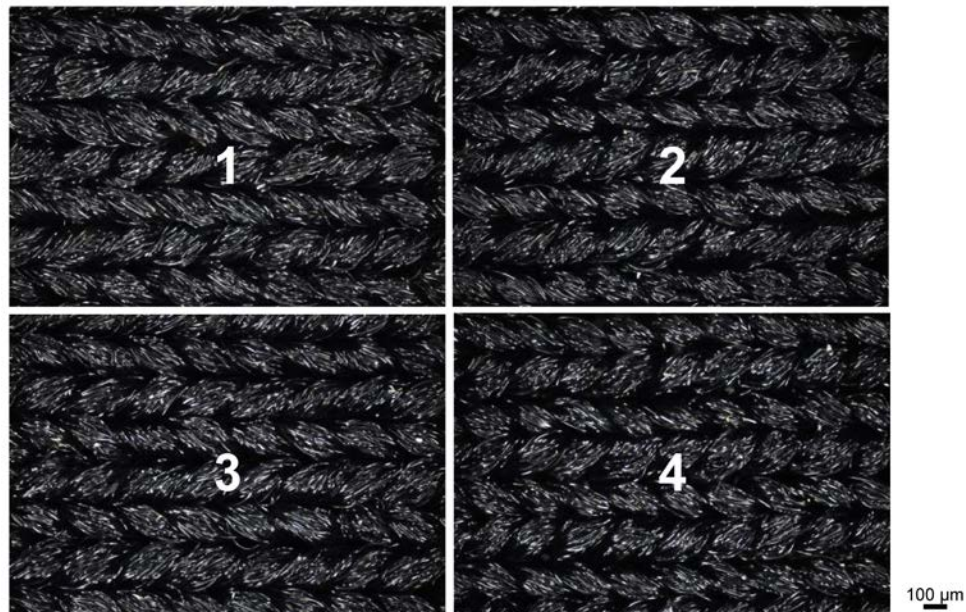


Fig. 1. Color optical microscope images of the fabric samples confirm that all samples have the same color and knit structure. Sample identifier numbers are overlaid in white.

### 3. Experimental details

Briefly, we used an MIR-sensitive camera to measure the infrared emission from a set of fabric samples as they were all held at the same temperature, as shown in Fig. 2. To obtain statistically significant results, we used temporal averaging over 50 images to reduce the effects of pixel noise and spatial averaging to reduce effects due to variations across fabric surfaces. Finally, the spatially and temporally averaged infrared emission values were used, in conjunction with measured values for blackbody and background ambient reflected radiation, to calculate the emissivity of each fabric sample.

#### 3.1. Experimental apparatus

As shown in Fig. 2(a), four fabric samples, nominally 32-mm-square swatches, were placed on a 152.4-mm-diameter copper disk, with all samples being placed at the same radial distance from the disk center and each sample positioned within its own 72° segment. A plate of polished brass (emissivity of 0.03 [9]) was placed in the remaining segment to act as a surface with approximately 100% reflectivity. To provide good thermal contact between the copper disk and the samples, the fabric and brass were adhered to the copper disk using thermal paste with a conductivity of 0.92 W/m•K. A uniform and consistent thickness of the thermal paste was ensured by first placing a thin template with a square cutout matching the dimensions of the fabric sample on the copper disk, then using a blade extended across the template to pull the paste down the application area. Upon removal of the template, a square section of paste with a thickness matching that of the template was left behind. To ensure that each fabric sample was placed on the thermal paste with uniform contact pressure, a 19-mm-thick copper square with dimensions matching that of the fabric sample was briefly placed on top of each fabric sample once it was situated on top of the thermal paste. To aid with the automatic image analysis described below, the brass plate was framed with high emissivity tape.

A circular resistive heating pad (Omega P/N SRMU0206D-P) with a diameter equal to that of the copper disk was placed under the copper disk and connected to a variable voltage supply (Payne Controls, McMaster-Carr P/N 3641K43). The cylindrical symmetry of the apparatus helped ensure that each sample position was exposed to nominally identical thermal conditions during the experiment. To confirm a uniform, and minimum in magnitude, radial temperature gradient, six high-aspect-ratio holes (3.18-mm diameter by 19-mm deep) were drilled into the 25.4-mm-thick copper disk: one in the disk center and five near the edge of the disk in the angular centers of each of the 72° segments. These holes acted as blackbody resonant cavities, with an effective emissivity of 1, and enabled accurate measurement of the local temperature and maximum possible (i.e., blackbody) emissive power of the heated copper disk. Using the measured cavity temperature of each hole, the maximum deviation in temperature from center to edge of the disk was measured to be less than 0.2°C for a nominal disk temperature of 35°C. The deviation in temperature between the outer holes in different segments was measured to be less than 0.1°C, confirming uniform thermal conditions for all sample positions.

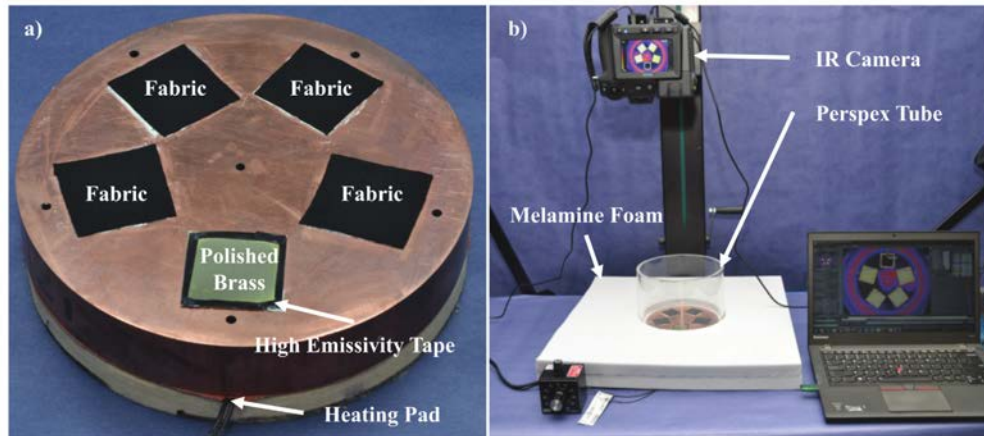


Fig. 2. Experimental apparatus: a) samples mounted to copper disk, four fabric samples containing different amounts of ceramic additive and one highly reflective brass plate are positioned around the disk at a constant radial distance; b) the copper disk within the measurement rig, an infrared camera is positioned above the disk, melamine foam reduces the radial temperature gradient of the copper and a clear acrylic tube limits convection.

Figure 2(b) shows the experimental apparatus configuration used for measurements. The copper disk was surrounded in melamine foam to reduce the radial temperature gradient, and a clear poly(methyl methacrylate) (PMMA) cylindrical tube was mounted around the copper disk to limit the effects of convective heat transfer in the vicinity of the samples. A scientific grade thermal imaging camera (FLIR Systems, Inc., Model T650sc, Wilsonville, OR) was mounted directly over the samples to acquire images at an angle normal to the surface of the copper disk. The camera was set to detect the radiance in the MIR wavelength range between  $7.5 - 14.0 \mu\text{m}$  using a  $640 \times 480$  array of microbolometer sensors with a pitch of  $25 \mu\text{m}$ , and the vertical distance between the camera and the samples was  $430 \text{ mm}$ .

### 3.2. Measurement methodology and image processing

With the samples mounted, the copper disk was heated to a nominal temperature of  $35^\circ\text{C}$  by adjusting the voltage controller. For these thin fabrics with a  $\sim 0.6\text{-mm}$  measured thickness, it was assumed that the temperature gradient across the thickness of the fabric could be neglected. At thermal equilibrium, the temperature of the fabric surface was taken to be equal to that of the copper disk, and differences in radiance measured were due solely to emissivity differences of the materials.

Once the copper disk and fabric samples reached a temperature of  $35^\circ\text{C}$  and stabilized for a minimum of 1 minute, a series of 50 images were acquired by the camera at a frequency of 7.5 Hz. The images were processed to create a single composite image in which each pixel is the mean radiance of the corresponding pixels in every image within the series. This process was used to temporally average the images, thereby smoothing out random noise fluctuations in the camera sensors to increase the signal-to-noise ratio.

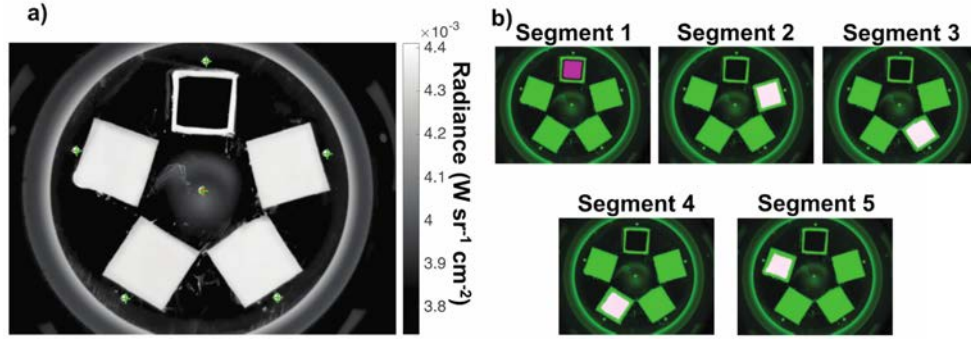


Fig. 3. Example composite radiance image and regions extracted for analysis: a) The fabric samples, cavity holes, and the tape framing the brass plate show up as regions of high radiance. The position of the cavity holes and the center of the copper disk, as detected by the automatic image analysis are indicated with green crosses and a red circle, respectively; b) The regions from which radiance data were extracted from each segment are indicated with fabric surface regions shown in white and the brass region shown in pink.

The spatial average of the radiance over the surface of each sample was extracted from the composite image via an image processing analysis technique. An example composite image is shown in Fig. 3(a), the location of the cavity holes and the disk center are indicated with green crosses and a filled red circle, respectively. Using the disk center, the copper disk was divided into equal-sized  $72^\circ$  segments that each contained one sample position. Thresholding and image masking techniques were used to extract and average the values of the pixels from each of the fabric samples and the brass plate. To avoid capturing any emission from the thermal paste, which can extrude slightly beyond the edge of samples, values near the edge of the sample regions were not included in the spatial averaging. Figure 3(b) shows the image from Fig. 3(a) with the regions from which radiance values were extracted for each of the fabric samples and the brass plate indicated. The spatial averaging, which reduces the measurement variation over the surface of the samples due to fabric sample properties, allowed an average value of detected radiance to be extracted from each fabric sample and the brass plate. In addition, the radiance values from the six cavity holes were calculated.

The emissivity of the fabric samples was calculated from the average detected radiance values. Other laboratory measurements have confirmed that the fabrics are opaque to this region of infrared radiation, so it is a valid assumption that no radiation from the copper disk penetrates the fabric. The detected radiance from a given fabric sample,  $W_d$ , was taken to be comprised of two components: radiation directly emitted by the fabric sample and ambient radiation that is reflected from the fabric sample. The radiance due to emission from the fabric is the product of the radiance of a black body at the sample temperature, taken as the average radiance from the cavity holes in the copper block, and the emissivity of each sample surface. The radiance due to the reflected ambient radiation,  $W_a$ , was calculated as the average detected radiance from the polished brass plate with a reflectivity of  $\sim 1$ . Thus, the emissivity of each fabric sample was obtained as

$$\begin{aligned}
 W_d &= \epsilon W_b + (1 - \epsilon) W_a \\
 \Rightarrow \epsilon &= \frac{W_d - W_a}{W_b - W_a},
 \end{aligned} \tag{3}$$

where  $\epsilon W_b$  is the component directly emitted by the fabric and  $(1 - \epsilon) W_a$  is the component reflected from the fabric sample due to ambient radiation from the surrounding environment. Note that as the sample temperature approaches the ambient room temperature,  $W_a$

approaches  $W_d$  and  $W_b$ , leading to a reduction in the signal-to-noise ratio for the measured emissivity. Thus, Eq. (3) dictates that measurements using this experimental method must be made at sample temperatures that are above or below the ambient room temperature.

The above experiment was repeated several times with different fabric samples in each position of the copper block. Since the magnitude of the measured changes in emissivity were small, the cumulative measured emissivity results were monitored, using the standard deviation for each fabric type, to estimate the reliability of the measured emissivity values as data were accumulated. After 12 experimental runs, it was determined that further repeated measurements were yielding little change to the average calculated emissivity of each sample and would therefore not increase the measurement reliability. For each experimental run, the location of the different samples was varied to ensure that any measured changes in infrared emissive power were not due to non-ideal cylindrical symmetry of the sample thermal environment.

#### 4. Results and discussion

Figure 4 shows the emissivity of the fabric samples as a function of the percentage mass of ceramic material in the fabric,  $x_c$ . The data points are the mean value of the 12 independent measurements and the error bars have a length of one standard deviation above and below the mean. A linear fit to the data yields a trend line described by  $\epsilon = 0.0148x_c + 0.9039$ , and the resulting line of best fit to these mean values, shown in black on the figure, has an  $R^2$  value of 0.976.

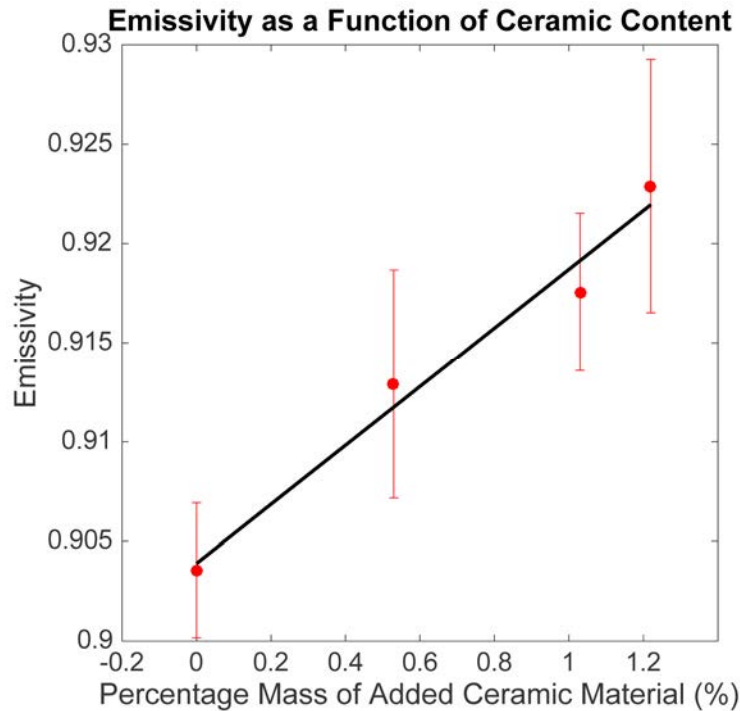


Fig. 4. Emissivity of the fabric samples as a function of the percentage mass of added ceramic material. Data points are the mean of 12 independent measurements and the error bars a range of one standard deviation above and below the data point values. The black line shows a linear fit to the data with an  $R^2$  value of 0.976.

The emissivity of the fabric is  $0.904 \pm 0.003$  when the fabric contains no added ceramic particles,  $0.913 \pm 0.006$  when the fabric contains  $0.53 \pm 0.03$  wt% added ceramic particles,

$0.918 \pm 0.004$  when the fabric contains  $1.03 \pm 0.06$  wt% added ceramic particles, and  $0.923 \pm 0.006$  when the fabric contains  $1.22 \pm 0.04$  wt% added ceramic particles. When ceramic material is added to be 1.22% of the fabric mass, the emissivity is increased by 2.1% over the case where no additional ceramic is added to the polyester/elastane blend.

The experimental methods described above were used to investigate the effects of temperature on the fabric sample that contained 1.22% added ceramic material by mass, achieved by mounting four samples of the 1.22% fabric on the copper disk, along with the high reflectivity brass plate. Figure 5 shows that the resulting emissivity is independent of temperature over the wavelength range of 7.5 – 14  $\mu\text{m}$ ; there is no statistically significant correlation between the emissivity and temperature with a p-value for linear correlation of 0.216.

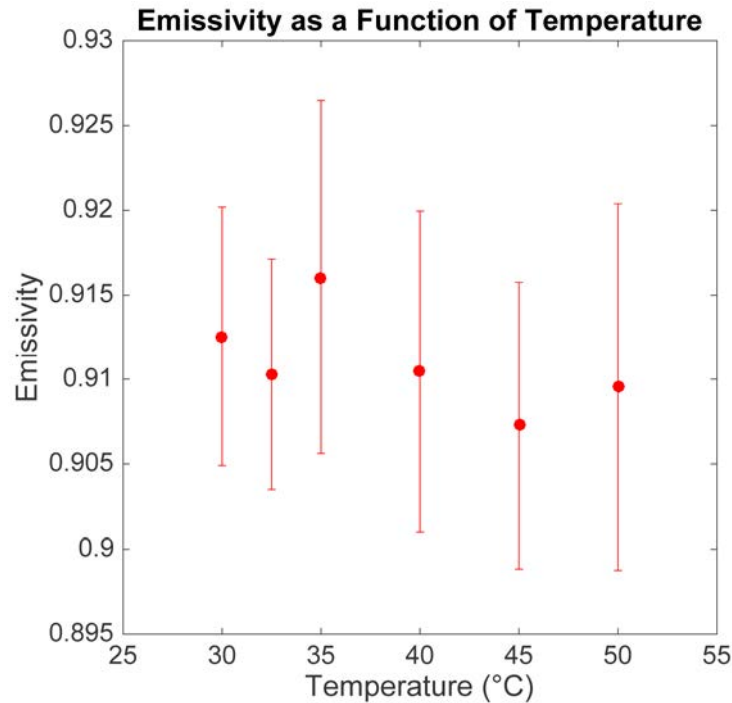


Fig. 5. Emissivity of the fabric containing 1.22% mass of added ceramic particles as a function of temperature over the wavelength range of 7.5 – 14  $\mu\text{m}$ .

These experiments center on the range of temperatures that may be encountered by fabrics in garments during typical wearing activities in temperate climates. The increase in emissivity as more ceramic is incorporated into the fabric, combined with the temperature-independent nature of the emissivity, offer encouragement that these results may be extrapolated to a broader range of scenarios involving more extreme temperature ranges and larger ceramic contents.

This methodology for measuring small variations in the emissivity of fabric surfaces, and possibly other surfaces, may find applications across a variety of fields ranging from textile technology to research into the properties and deposition of thin-film materials. An immediate application of this work is to use the techniques detailed above to investigate the emissive properties of other fabrics, such as cotton or man-made fibers. This could enable, for example, effects on the thermal performance of garments due to modifications of fabric structure, surface texture or coating, and fiber or additive content, to be assessed. In addition, such investigations could be used to optimize fabric structure or composition for use in specific thermal conditions.

## **Acknowledgments**

Partial funding for this work was provided by Hologenix, LLC (Santa Monica, CA). We thank Ke Zhao (Exponent, Inc., Menlo Park, CA) for fruitful discussions regarding the statistical significance of the data, and Dr. Scott Seidel (Exponent, Inc., Atlanta, GA) for organizing the ash analysis of the fabric samples.